RevMexAA (Serie de Conferencias), **1**, 347-354 (1995)

HIGH ANGULAR RESOLUTION IMAGING OF CIRCUMSTELLAR ENVIRONMENT OF YOUNG STARS

Fabien Malbet
Laboratoire d'Astrophysique, Observatoire de Grenoble, BP 53, F-38041 Grenoble cedex 9, France

RESUMEN

Durante la última década se ha encontrado una gran cantidad de evidencia indirecta sobre la presencia de discos circunestelares alrededor de objetos estelares jóvenes. Además, en el entorno de los discos circunestelares, se han descubierto compañeras múltiples, chorros ópticos y envolturas de discos. Sólo observaciones con resoluciones angulares mejores que 0.″1 desenmarañarán la estructura interna de este entorno tan complejo, y proveerán pruebas directas sobre la presencia de discos protoplanetarios. La interferometría de motas, óptica adaptativa e interferometría con apertura múltiple en el rango visible y cercano infrarrojo nos permitirá alcanzar esa resolución angular. Presentaré diversas observaciones de interferometría de motas, así como observaciones realizadas con óptica adaptativa, llevadas a cabo con el prototipo VLT del sistema de óptica adaptativa *COME-ON+* y obtenidas por el Observatoire de Grenoble en objetos estelares jóvenes. También presentaré una discusión sobre las razones del porqué es tan difícil detectar estructuras extendidas, como son los discos, con las técnicas actuales.

ABSTRACT

Over the past decade, much evidence although indirect for the presence of circumstellar disks around young stellar objects has been found. However the observations of the circumstellar environment have always revealed a much more complex picture. In addition to the presence of circumstellar disks, multiple companions, optical jets, disk envelopes have been discovered. Only observations allowing resolution better than 0.1 arcsec will unravel the inner structure of this complex environment and will provide direct evidence for the presence of protoplanetary disks. High angular resolution techniques such as speckle interferometry, adaptive optics and multi-aperture interferometry in the visible and near-infrared range allow us to reach this requested high spatial resolution. I will present the current status of various speckle observations and adaptive optics observations carried out with the VLT prototype of adaptive optics system COME-ON+ obtained by the Observatoire de Grenoble on young stellar objects. I will also present a discussion on the reasons why it is so difficult to detect extended structures like disks with the current state of art. In order to study extended structures close to the star, observations require high dynamic range techniques like coronography coupled with high angular resolution instruments for the scattered light, and, near infrared long baseline interferometry for the disk thermal emission.

Key words: **ACCRETION, ACCRETION DISKS — TECHNIQUES: INTERFEROMETRIC — STARS: CIRCUMSTELLAR MATTER — STARS: IMAGING — STARS: PRE-MAIN SEQUENCE**

1. INTRODUCTION - OBJECTIVES

T Tauri stars are low-mass stars in the early stage of their evolution. Some materials remain from the collapse of the genitor cloud which are either falling onto the central star by accretion or ejected outwards by stellar winds or bipolar jets. There is some observational evidence for the presence of circumstellar material around T Tauri stars, but most of it is indirect. Most of these materials are found around the so-called classical T Tauri stars (CTTSs) rather than around the weak-line T Tauri stars (WTTSs). In this paper, I will address mainly the case of CTTSs.

Photometric observations have shown that spectral energy distributions of young stars have both ultraviolet and infrared excesses. This has been successfully interpreted by the presence of an accretion disk about 100 AU in size. The infrared excess comes from the radiation of the cold outer parts of the disk and the ultraviolet excess from the hot inner boundary layer between the disk and the star (Bertout, Basri, & Bouvier 1988; Basri & Bertout 1989).

Spectroscopic observations have revealed the "veiling" of optical spectrum which fills most of the absorption lines. The most commonly assumed interpretation is the contribution of disk boundary layer continuum to the stellar continuum which decreases the equivalent width of the lines. Furthermore, forbidden line profiles, which are shaped in the outer parts of the ionized stellar wind, are often blueshifted with little or no emission on the red line side. This phenomenon is well understood with the disk model because the disk obscures the red receding part of the wind (Appenzeller et al. 1984, Edwards et al. 1987).

Polarimetric observations show that a large fraction of the CTTSs have large amount of intrinsic polarisation (more than 1%). A frequent explanation is the presence of a optically thick disk and an optically thin envelope in the circumstellar medium. The stellar photons are scattered several times in the disk and therefore get a polarization which is parallel to the disk plane if the disk is seen edge-on. Polarization maps give better details that confirm the interpretation (Bastien & Ménard 1990).

Disks are not the only material around young stars. Without getting into details, circumstellar environments of young stars have jets and envelopes, and very often T Tauri systems are multiple. One of the most interesting question is to understand the correlation between accretion and ejection, disks and jets, as observationally revealed by Cabrit et al. (1990). This connection under theoretical study (Shu et al. 1994, Ferreira & Pelletier 1994) will be fully understood when observations of the very close environment will be possible. High angular resolution techniques are therefore very important to probe the circumstellar medium of T Tauri stars.

This paper presents the current results of high angular resolution imaging in TTS field, and shows the steps toward better resolution and dynamic range in order to increase the number of observations and their quality.

2. HIGH ANGULAR RESOLUTION TECHNIQUES

2.1. Image Formation at Optical Wavelengths

The theoretical limit for the resolution of a telescope of diameter D is about λ/D. With current telescope size ($D = 4$ m), at $\lambda = 2.2\ \mu$m the resolution should be $R \approx 0.1''$. At $\lambda = 0.5\ \mu$m the resolution should be $R \approx 25$ mas (1 mas = $0\farcs001$). Unfortunately the actual resolution is closer to $1'' - 2''$, because of the atmospheric turbulence. This corresponds to a telescope diameter of $r_0 = 10$ cm in at $\lambda = 0.5\ \mu$m.

What happens is that the coherence of the stellar wavefront arriving on the telescope aperture is reduced to the size, r_0, of the atmospheric turbulence cells (thermal instability). The wavefront instead of being perfectly plane is rippled. At the scale of the turbulence cells the wavefront looks plane but randomly tilted. A simple and reduced interpretation of the image is the sum of the multiple images of the star with random phase differences. The result at exposure time shorter than the turbulence timescale is a pattern of speckles. Individual speckles have a characteristic size λ/D even though the characteristic size of the global pattern is λ/r_0. Taking long exposure gives seeing-limited images with gaussian-like shape and λ/r_0 resolution (Roddier 1979). Figure 1 show the representation of the stellar image at short exposure and long exposure. High angular resolution techniques provide ways of recovering full spatial resolution and therefore are a powerful way to investigate the close environment of young stars.

2.2. High Angular Resolution Techniques

Present regularly-used techniques in the high angular resolution field are speckle interferometry and adaptive optics. The goal of this paper is not to give a review of these techniques, but to introduce them to the star formation community and present current observations. For more information, reviews by Labeyrie (1978) and Chelli (1984) for speckle interferometry and Beckers (1993) for adaptive optics are recommended.

Speckle interferometry records images taken with short exposure times in order to freeze the atmospheric turbulence. Fourier transforms are computed, and amplitudes and phases are carefully averaged. The visibility

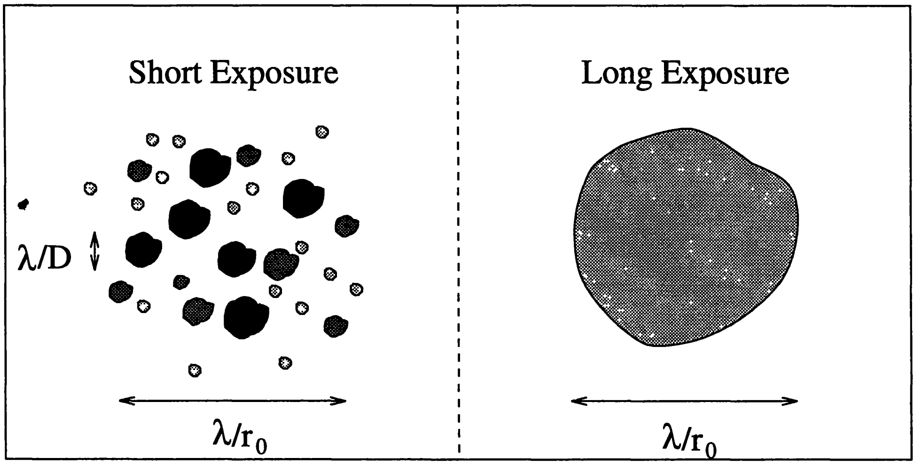

Fig. 1.— Short exposure vs. long exposure in image formation.

is the ratio between the averaged Fourier transform of the object image and the averaged Fourier transform of the image of a reference star which calibrates the intrinsic response of the telescope. The visibility is only defined in the range of the telescope spatial frequencies. A careful inverse Fourier transform of the visibility gives a reconstructed image of the object.

Adaptive optics is a real-time correction technique. Figure 2 gives a schematical representation of how adaptive optics works. The star beam is collimated so that the perturbated wavefront can be reflected on a deformable mirror conjugated with the telescope primary mirror. A beamsplitter then separates the beam into a science beam and a beam for the wavefront sensor. The wavefront sensor measures the deformation of the wavefront. A computer calculates the deformation to be applied onto the deformable mirror in order to correct the wavefront. A servo-loop is generated and the bandwidth must be such that the correction time is smaller than the turbulence characteristic time. In fact the wavefront after reflection onto the deformable mirror is almost perfect and the wavefront sensor only measures the residual errors. The science beam is almost diffraction limited. As a matter of fact, the quality of the correction depends both on the number of actuators of the mirror, the temporal bandwidth and the seeing conditions. The correction is partial when the hardware/software cannot reach a perfect adequation with the weather conditions. However partial corrections without giving diffraction-limited images brings an outstanding improvement in spatial resolution. In this case, thanks to speckle-like techniques and to a reference star, diffraction-limited reconstructed images can be obtained with more sensitivity since the constraints are smaller (longer exposure time, phases less perturbated).

3. CURRENT OBSERVATIONS

This paper is supposed to present personal research and not review the state of the art. I will not address world-wide work on the subject but present observations and studies carried out by the "Young Stars Group" at the Observatoire de Grenoble.

3.1. Instruments

Table 1 summarizes the instruments used for speckle interferometry. Column 1 gives the name of the instrument, column 2 the reference for the instrument description, column 3 the wavelengths, column 4 the camera specification and column 5 the telescope.

Table 2 summarizes the instruments used for adaptive optics observations. Column 1 gives the name of the instrument, column 2 the reference for the instrument description, column 3 the wavelengths, column 4 the camera specification, column 5 the telescope and column 6 the number of actuators of the deformable mirror.

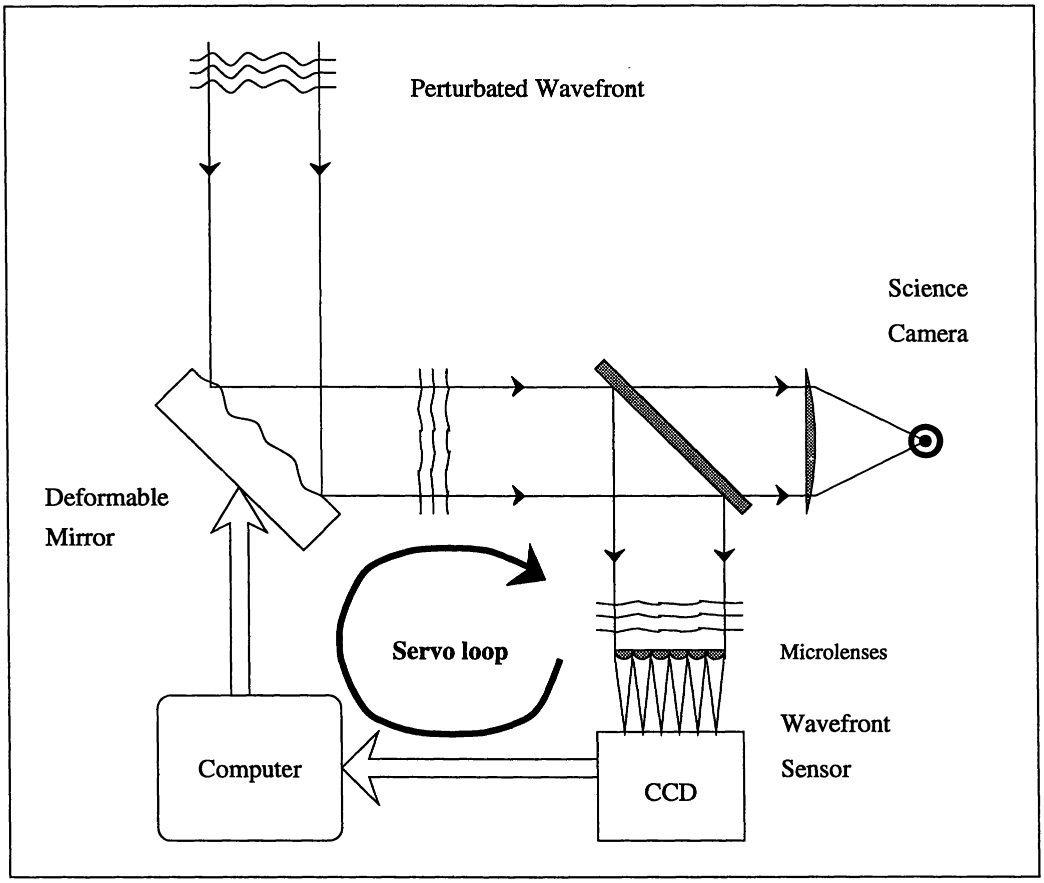

Fig. 2.— Adaptive optics principle.

3.2. Targets and Results

The goal of these observations was to find direct evidences for circumstellar material and search for companions. Targets were T Tauri stars, FU Orionis stars and Herbig Ae/Be stars. Results are summarized briefly and references are given when available for complementary information.

3.2.1. T Tauri Binaries

Tessier, Bouvier, & Lacombe (1994) have surveyed a small sample of T Tauri stars, most of which have flat infrared excess, in K, L', M bands with the *CIRCUS* 32 × 32 camera in speckle mode. With the resolution of the 3.6-m *Canada-France-Hawaii* telescope, results show that FS Tau, HL Tau, RY Tau, GK Tau and GI Tau are unresolved, DD Tau, T Tau and UY Aur are resolved as binaries. These observations suggest that XZ Tau and DO Tau are partially resolved.

T Tau has also been observed with Foy's specklegraph in the Hα line at the *CFH* telescope by Devaney et al. (1995). The authors found an elongation of $\approx 0\farcs09$ at P.A. $192 \pm 5°$ and argue that this emission arises either from the interaction between a weakly collimated wind with a circumstellar flaring disk, or from the basis of the westward jet seen on a larger scale.

3.2.2. DF Tau

The case of DF Tau is interesting. Chen et al. (1990) observed this star by lunar occultation and found it binary. Thiébaut (1994) and Thiébaut et al. (1994) have observed this binary at two different epochs 1989.84

Table 1.— Speckle instruments used for the observations.

Instrument	Reference	Wavelength	Camera	Telescope
Specklegraph	Foy (1988)	Visible	CP40, photo- -counting camera	CFHT, Russian SAO
Circus 32×32, speckle mode	Lacombe et al. (1989)	K, L', M	InSb 32×32	CFHT
Circus 128×128, speckle mode	Lacombe et al. (1992)	K, L', M	InSb 128×128	CFHT
SHARP	Hofman et al. (1992)	J, H, K	Nicmos 3 256×256	ESO NTT

Table 2.— Adaptive optics systems used for the observations.

Instrument	Reference	Wavelength	Camera	Telescope	Actuators
HR Cam	Racine & McClure (1989)	Visible	CCD $2k \times 2k$	CFHT	2 (tip-tilt)
COME-ON	Rigaut et al. (1991)	K, L', M	Circus 32×32	3.6-m ESO	19
COME-ON+	Beuzit et al. (1994)	J, H, K	SHARP II	3.6-m ESO	49

and 1991.73 with their specklegraph at the 3.6-m *CFH* telescope and the 6-m Russian *SAO* telescope and found that the separation and the position angle has changed. These motions are interpretated as orbital motions. The deduced period of this orbit is 80 ± 5 yrs and the major axis 16.3 ± 0.5 AU (DF Tau lies at 140 pc). These parameters allow the authors to compute the dynamic masses which are $M_1 + M_2 \approx 0.7 \pm 0.2$ $M_\odot$.

3.2.3. NX Pup

NX Pup has been observed by the adaptive optics system COME-ON+ (Brandner et al. 1994, Tessier et al. 1994) and found to be triple. In addition to separation, position angle and brightness ratio measurements in the J, H, K bands, spectroscopy of OI, IIα, Hβ, Hγ and LiI (λ = 6708 Å) have been performed. All this information allowed the author to locate the different stars, NX Pup A, NX Pup B and NX Pup C on the Hertzprung-Russell diagram and obtain an estimate of their ages and masses. NX Pup A is approximately 5.10^6 yrs old and 2 $M_\odot$ massive, NX Pup B $0.3 - 5.10^6$ yrs old and $2 - 2.5$ $M_\odot$ massive and NX Pup C 5.10^5 yrs old and 0.3 $M_\odot$ massive. This would be the first low-mass T Tauri star detected in this cometary globule.

3.2.4. Haro 6–10

Most of the observations show evidence for multiplicity in T Tauri systems. In Haro 6–10, Ménard et al. (1993, posters A47 and B14 in this conference) have found evidence for circumbinary material. Haro 6–10 has been observed with *CIRCUS* 128×128 at the 3.6-m *CFH* telescope in K, L, M bands. The binary nature previously found by Leinert & Haas (1989) is confirmed with separation of 1″.25, and position angle of 355°. 5.7% of linear polarization is measured at P.A. 89°, almost perpendicular to the line joining the two stars and is interpreted by the presence of a flat structure around the two stars, perhaps a circumbinary disk. Recent millimeter observations with the *Plateau de Bure* interferometer (Monin et al., private communication) support this result by resolving the circumbinary envelope.

3.2.5. Z CMa

Z CMa is a famous FU Orionis system. Many speckle works have observed the binary nature of Z CMa in J, H, K bands. Malbet et al. (1993) have confirmed by using COME-ON the ESO VLT adaptive optics prototype in L', M bands that Z CMa was binary, but also found the presence of a 400 AU disk-like structure around the infrared northern star. This observation was obtained at the limit of diffraction and has to be confirmed. Tessier, Bouvier, & Lacombe (1994) have observed this FU Orionis system also in L', M bands, but with *CIRCUS* 128×128 in speckle mode. No evidence of disk was found. Observations by Roddier et al. (1994) in J, H with their adaptive optics system show that the component formerly the brightest has become the faintest. As a FU Orionis star, Z CMa is a very variable source and an explanation for the disk structure might be an accretion burst. Very recently, Thiébaut (1994, also Thiébaut et al. 1994) have detected the so-called infrared north-western companion at visible wavelengths (636 nm and 730 nm) with their specklegraph at the 3.6-m *CFH* telescope. This detection can be explained by the scattered polarized light of the infrared companion detected by Whitney et al. (1993). Barth, Weigelt, & Zinnecker (1994) have found the same result with speckle masking techniques.

3.2.6. Cepheus OB IV Association

Ménard, Wöhler, & Monin (1995) have used *HR Cam* at the 3.6-m *CFH* telescope at visible wavelengths in order to detect circumstellar nebulosities around highly polarized young stellar objects. In the Cepheus OB IV association, they detected nebulosities around 3 among 5 stars. These objects have infrared excess, high polarization, circumstellar matter but are not very active since no jets and no Herbig Haro objects have been detected.

4. DETECTING EXTENDED STRUCTURE

In most results presented in this paper, high angular resolution techniques have failed to detect extended circumstellar structure (except for Z CMa, but the disk-like structure found by Malbet et al. 1993 has yet to be confirmed). This remark is also representative of world-wide results. In millimeter and sub-millimeter wavelengths, few extended structures have been discovered: a rotating ring around GG Tau (Dutrey, Guilloteau, & Simon 1994), circumstellar disks around HL Tau and L1551 (Lay et al. 1994, Carlstrom in his Conference talk).

Why can we not detect extended structure in optical wavelength? The answer may be found in the analysis of the origin of light radiation. The two expected contributions from the circumstellar material are the thermal emission and the scattered light.

4.0.7. Thermal Emission

Concerning the thermal emission, there are two regimes corresponding to the two parts of black-body emission: the Wien approximation where the change in flux is exponential and the Rayleigh-Jeans approximation where the change follows a power law. The transition is given by the maximum flux of the black-body:

$$\lambda T = 3000\ \mu\text{m K} \tag{1}$$

If we assume a radial distribution of temperature varying as a power law as suggested by studies of far infrared spectral energy distribution (Adams, Emerson, & Fuller 1990; Beckwith et al. 1990),

$$T = T_0 \left(\frac{r}{r_0}\right)^{-q} \tag{2}$$

we get for the radial distribution of the intensity, $I(r)$, in the disk:

$$\text{if } \frac{T}{1500\text{K}} \leq \frac{\lambda}{2\ \mu\text{m}} \quad \text{then} \quad I(r) \propto e^{-Kr^q} \tag{3}$$

$$\text{if } \frac{T}{1500\text{K}} \geq \frac{\lambda}{2\ \mu\text{m}} \quad \text{then} \quad I(r) \propto r^{-q} \tag{4}$$

The disk is hotter than 1000 K only in the inner part of the disk ($r \leq 0.05$ AU). The exponential regime decreases too quickly to be detectable, therefore only very high angular resolution as long-baseline interferometry would be able to detect thermal emission from T Tauri disks. Some simulations presented by Malbet & Bertout (1995; also Bertout, Reipurth, & Malbet 1994) show that thermal emission is detectable at wavelengths larger than 2.2 μm.

4.0.8. Scattered Light

Part of the stellar light is scattered through the disk. As a matter of fact, it can be simple scattered in optically thin regions and multiple scattered in optically thick regions. If we consider a simple optically thin

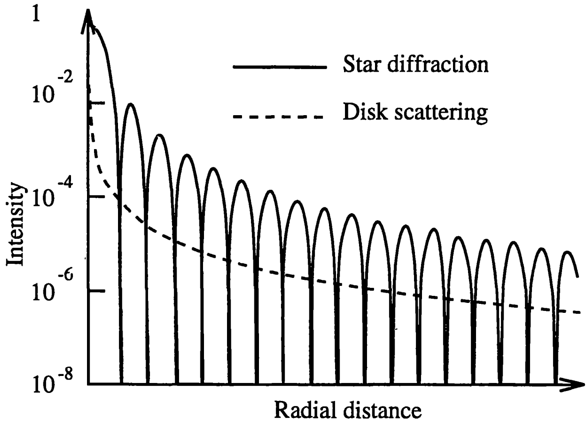

Fig. 3.— Disk extended emission vs. star diffraction.

geometrically flat disk, the radial distribution of the intensity is proportional to the dilution factor (Mihalas 1978),

$$W(r) = \frac{1}{2}\left(1 - (1 - \frac{r}{R_*})^{-2}\right)^{1/2}, \tag{5}$$

which approximatively varies proportionally to $(r/R_*)^{-2}$ when $r \gg R_*$ (r is the projected distance to the star, R_* the star radius).

The main problem is the background generated by the wing of the diffraction pattern. The radial dependence of the diffraction pattern, $I_*(r)$,

$$I_*(r) = \left(\frac{2J_1(\pi\frac{Dr}{\lambda d})}{\pi\frac{Dr}{\lambda d}}\right)^2 \tag{6}$$

is in general much brighter than $I(r)$ (see Fig. 3). The maxima of $I_*(r)$ varies asymptotically as r^{-3} when $r/d \gg \lambda/D$ (d the distance of the source, D the telescope diameter, λ the wavelength).

This shows that if the telescope is perfect (no phase errors on the mirrors) we can detect the disk contribution if we look far enough from the central star. To detect a faint scattering disk, we need to decrease the star diffraction. This can be achieved with coronographic techniques (Malbet 1995) coupled with high angular resolution.

5. FUTURE PROSPECTS IN DISK IMAGING

Extended structures around young stars are certainly faint. The thermal emission is concentrated in the inner part of the disk and emits in the infrared. The scattering light has a wider effect around the star, but has a fainter contribution compared to the star. Proposed ways to detect disk extended emission are the promising optical long-baseline interferometry in the near infrared (e.g. the VLT Interferometer, cf. Malbet 1994; Malbet & Bertout 1995) and adaptive optics coronographs. The previous technique will permit to detect mainly thermal emission from the disk and the latter will permit to observe wide scattered stellar radiation in the disk. Thermal emission will give information on the disk photosphere and scattered emission on the upper disk chromosphere.

We would like to thank N. Ageorges, J. Bouvier, F. Ménard, J.-L. Monin, E. Tessier, E. Thiébaut for providing nice images of their observations and useful comments for the talk. I would like also to thank C. Bertout, J. Bouvier, F. Ménard, J.-L. Monin for commenting the paper.

REFERENCES

Adams, F. C., Emerson, J. P., & Fuller, G. A. 1990, ApJ, 357, 606
Ageorges, N., Ménard, F., Monin, J.-L., & Eckart, A. 1994, A&A, 283, L3
Appenzeller, I., Jankovics, I., & Oestreicher, R. 1984, A&A, 141, 108
Barth, W., Weigelt, G., & Zinnecker, H. 1994, A&A, 291, 500
Basri, G., & Bertout, C. 1989, ApJ, 341, 340
Bastien, P., & Ménard, F. 1990, ApJ, 364, 232
Beckers, J. M. 1993, ARA&A, 31, 13
Beckwith, S. V. W., Sargent, A. I., Chini, R. S., & Güsten, R. 1990, AJ, 99, 924
Bertout, C., Basri, G., & Bouvier, J. 1988, ApJ, 330, 350
Bertout, C., Reipurth, B., & Malbet, F. 1994, in ESO Workshop Science with the VLT, ed. J. Danziger & J. Walsh, in press
Brandner, W., Bouvier, J., Grebel, et al. 1994, A&A, in press
Cabrit, S., Edwards, S., Strom, S. E., & Strom, K. M. 1990, ApJ, 354, 687
Chelli, A., 1984, in Very Large Telescopes, Their Instrumentation and Programs, IAU Col. 79, 309
Chen, W. P., Simon, M., Logmore, A. J., Howell, R. R., & Benson, J. A. 1990, ApJ, 357, 224
Devaney, M. N., Thiébaut, E., Foy, R., et al. 1995, A&A, in press
Dutrey, A., Guilloteau, S., & Simon, M. 1994, A&A, 286, 149
Edwards, S., Cabrit, S., Strom, S., et al. 1987, ApJ, 321, 473
Ferreira, J., & Pelletier, G. 1994, A&A, in press
Labeyrie, A. 1978, ARA&A, 16, 77
Lay, O. P., Carlstrom, J. E., Hills, R. E., & Phillips, T. G. 1994, ApJ, 434, L75
Leinert, C., & Haas, M. 1989, ApJ, 342, L39
Malbet, F. 1994, in Astrophysical programs for VISA, ed. J. Bouvier & F. Vakili
Malbet, F. 1995, A&A, submitted
Malbet, F., & Bertout, C. 1995, A&A, submitted
Malbet, F., Rigaut, F., Bertout, C., & Léna, P. 1993, A&A, 271, L9
Ménard, F., Monin, J.-L., Angelucci, F., & Rouan, D. 1993, ApJ, 414, L117
Ménard, F., Wöhler, C., & Monin, J.-L. 1995, A&A, in preparation
Mihalas, D. 1978, in Stellar Atmospheres, ed. Freeman and Company (San Francisco), 120
Roddier, F. 1979, J. Opt. (Paris) 10, 299
Roddier, F., Anuskiewicz, J., Graves, J. E., Northcott, M. J., & Roddier, C. 1994, SPIE, 2201, 01
Shu, F. H., Najita, J., Ostriker, E., et al. 1994, ApJ, 429, 781
Tessier, E., Bouvier, J., & Lacombe, F. 1994, A&A, 283, 827
Tessier, E., Bouvier J., Beuzit, J.-L., & Brandner, W. 1994, The ESO Messenger, 78, 35
Thiébaut, E. 1994, PhD thesis, Université Paris 7 (France)
Thiébaut, E., Bouvier, J., Blazit, A., et al. 1994, A&A, submitted
Whitney, B. A., Clayton, G. C., & Schulte-Ladbeck, R. E., et al. 1993, ApJ, 417, 687